DESIGN AND TRANSPORT PROPERTIES OF (ETHYLENE GLYCOL + WATER)-BASED NANOFLUIDS CONTAINING GRAPHENE NANOPLATELETS

Cabaleiro D.[1], Colla L.[2], Barison S.[3], Lugo L.[1*], Fedele L.[2], Bobbo S.[2]

[1]Departamento de Física Aplicada, Facultade de Ciencias,
Universidade de Vigo
Vigo, Spain

[2]Istituto per le Tecnologie della Costruzione
Consiglio Nazionale delle Ricerche
Padova, Italy

[3]Istituto per l'Energetica e le Interfasi
Consiglio Nazionale delle Ricerche
Padova, Italy

*E-mail: luis.lugo@uvigo.es

ABSTRACT

In this work, stable homogeneous nanofluids were designed as dispersions of sulfonic acid-functionalized graphene nanoplatelets in an (ethylene glycol + water) mixture at (10:90)% mass ratio and nanoparticle mass concentrations up to 0.5 wt.%. Nanofluid stability was evaluated by means of Dynamic Light Scattering (DLS) and Zeta Potential measurements. The thermal conductivity and dynamic viscosity of base fluid and nanofluids were experimentally obtained in the temperature range from (283.15 to 343.15) K by using a TPS 2500S Hot Disk and an AR-G2 rotational rheometer, respectively. Thermal conductivity improvements reach up to 5% while the maximum dynamic viscosity increase is 12.6%. Finally, the experimental values of these two transport properties were also utilized to analyze nanoparticle concentration effect on heat transfer performance and pumping power through different figures of merit.

NOMENCLATURE

AAD%		Average Absolute Deviation
c_p	[J/g·K]	Specific heat capacity
EG		Ethylene glycol
GnP		Graphene nanoplatelet
GOnP		Graphene oxide nanoplatelet
k	[W/m·K]	Thermal conductivity
L_{ii}, β_{ii}		Coefficients of Nan model
Mo		Mouromtseff number
T	[K]	Temperature
W		Water
$\dot{W}$	[W]	Pumping power
η_0, D, T_0		Adjustable parameters of Vogel-Fulcher-Tamman (VFT) model

Special characters

$/\eta/$		Intrinsic viscosity
η	[mPa·s]	Dynamic viscosity
ρ	[g/cm^3]	Density
φ	[-]	Mass fraction, wt.%
ϕ	[-]	Volume fraction, vol%

Subscripts

bf	Base fluid
nf	Nanofluid
np	Nanoparticle

INTRODUCTION

The exponential growth in energy consumption experimented in the last few decades of the twentieth century has made evident the need to improve the thermal performance of thermal facilities in general and the weak heat-transfer abilities of most conventional heat transfer fluids in particular. In this sense, the suspension of nanoparticles in these conventional fluids, also called nanofluids, has become a subject of intensive study worldwide due to their anomalous thermal behavior [1].

Among the different nanoadditives utilized to engineer nanofluids, carbon nanostructures seem to exhibit the highest potential [2]. Within the family of graphite carbon allotropes, graphene (ideally envisaged as a single-atom-thick sheet of sp^2-bonded carbon atoms arranged in a honeycomb lattice) has raised great interest because of their exceptional mechanical, thermal, and electrical properties [3-4]. This two-dimensional material is commercially available in the form of stacks, with between 10 and 100 layers, known as graphene nanoplatelets or nanosheets (GnPs). GnPs exhibit not only thermal conductivities much higher than those of multi- or single-wire nanotubes, but also larger surface areas which favors a better contact area/interface with base fluid reducing Kapitza resistance [5]. These features, together with the relative easy and cost effective of producing GnPs make this material an excellent candidate as nanoadditive to develop nanofluids with improved thermal conductivities.

Graphene is hydrophobic and consequently it cannot be dispersed in water for a long time without agglomerate. However, stable suspensions in water or some organic solvents can be prepared by means of proper sonication once the material has been functionalized [6-7]. Surfactant addition and acid treatment are common methods to improve interactions between graphene nanostructures and base fluid necessary to prevent nanoparticle settling. Graphene functionalization by acid treatment can avoid the rise in pumping power due to the viscosity increase usually produced by the addition of surfactant. However, oxidation by acid can introduce defect

sites within the graphene structure of the nanosheets, which in turn can lead to a reduction in thermal conductivity [8-9]. Another peculiar property of graphene oxide (GO) is the high natural acidity of its aqueous solutions which must be controlled to prevent possible damages to metallic components in thermal facilities [10-11].

The thermal conductivity k, of nanofluids has attracted a lot of attention in last decades due to the significant influence of this property on heat transfer performance [12]. However, other properties such as density ρ, specific heat capacity c_p, and especially dynamic viscosity η, are necessary to make technical calculations. Furthermore, an analysis of different figures of merit (FoMs) based on these thermophysical properties, such as the Mouromtseff number (Mo) [13], can assist to compare the heat transfer capabilities of different heat transfer fluids [14].

Graphene nanofluids using water (W) [1, 15-18] or ethylene glycol (EG) [10, 17-19] have been largely studied in literature while (ethylene glycol + water) mixtures are preferred in many industrial installations since they combine the higher thermal conductivities of water with the lower freezing points of glycols. Up to our knowledge, only Kole and Dey [5], Amiri et al. [20], and Ijam et al. [21] have studied the thermophysical and rheological behavior of GnPs nanofluids in (EG+W) mixtures at 70, 60 and 40% in volume of EG, respectively.

This investigation deals with dispersions of acid-functionalized graphene nanoplatelets in an (ethylene glycol + water) mixture at (10:90)% mass ratio and nanoparticle mass concentrations of 0.1, 0.25 and 0.5%. Higher nanoadditive mass concentrations were not considered in order to ensure good nanoparticle stability and avoid higher viscosity penalties. Zeta potential and temporal variation of average nanoparticle size were analyzed with the aim of optimizing the preparation conditions such as sonication time or pH-value. The thermal conductivity and dynamic viscosity of nanofluids and base fluid were experimentally obtained, analyzing temperature and nanoparticle concentration dependences. The experimental values of these two transport properties were also used to assess how nanoparticle concentration influences on heat transfer performance and pumping power by means of different figures of merit.

EXPERIMENTAL

Materials

Sulfonic acid-functionalized graphene nanoplatelets (GOnPs) were provided by NanoInnova Technologies S.L (Madrid, Spain, www.nanoinnova.com). Ethylene glycol (Sigma-Aldrich, 99.5%) and reagent-grade water (18.2 MΩ·cm resistivity at 298.15 K) produced by means of a Millipore system (Billerica MA, USA) were utilized to prepare the base fluid, an (ethylene glycol + water) mixture at (10:90)% mass ratio. An ammonium hydroxide solution (30-33% NH_3 in water) from Sigma-Aldrich was used to modify the pH-value. Reagents were weighted in a Sartorius analytical balance with an uncertainty of 0.0001 g.

Nanofluid preparation and stability characterization

Nanofluids were designed following a two-step method. Hence, the amount of graphene nanopowder necessary to obtain the required nanoparticle concentration was first added to the base fluid and then stirred for 120 min. Afterwards, samples were sonicated by means of a CP104 Ultrasonic Bath (CEIA, Italy) operating at a power level of 200 W and a frequency of 40 kHz. As pointed out, the dispersion of GOnPs in aqueous solutions leads to a diminution in the pH-value. In our case, samples exhibit pH-values between 2.2 and 2.8. With the aim of selecting the optimum preparation conditions, the influence of pH-value and sonication time on nanofluid stability were evaluated through zeta potential and size measurements by means of a Zetasizer Nano (Malvern, U.K.) [22].

Firstly, zeta potential was studied as a function of pH for the 0.1% and 0.25% nanoparticle mass concentrations. Ammonium hydroxide was added to dispersions in order to obtain pH-values up to 10. No zeta potential measurements were performed for the highest mass concentration since detected intensity was outside optimum working conditions. Zeta potential remains constant around 40-43 mV for the pH range from 2.2 to 5 and then decreases as pH-value rises. The iso-electric point takes place at around 9.5. pH= 5 was selected to prepare the nanofluids in order to ensure zeta potentials high enough to ensure strong electrical repulsion charges around the particles and, at the same time, avoid possible future corrosion of metallic elements in facilities.

The nanoparticle size distribution of the dispersions was studied at 298.15 K by analyzing the random changes in the intensity of scattered light collected at an angle of 173°. It must be pointed out that sizing measurements obtained by means of dynamic light scattering (DLS) are based on the assumption that particles are spherical while the studied nanoadditives are sheet-like shaped. Apparent size measurements were performed for nanofluids designed using a 0.1% mass concentration of GOnP and sonication times ranging from (0 to 300) min. The studied GOnP/(EG+W) nanofluids exhibit a trimodal distribution with apparent sizes from a few nanometers to 4 μm. The average value and width of the different peaks reduce as sonication time increases, especially between (0 and 240) min. However, only little difference was found between samples using (240 and 300) min. Thus, larger sonication times were not considered and nanofluids at the three studied nanoadditive concentrations were prepared sonicating for 300 min.

Afterwards, nanofluid stability was analyzed with the time elapsed after preparation following the procedure proposed by Fedele et al. [22]. Hence, two different cuvettes were filled with each of the three concentrations and their apparent sizes were studied by DLS for a month. One of the two cuvettes was maintained in static conditions in order to assess the changes in size distribution due to natural sedimentation, while the other sample of the pair was periodically measured after manually shaking so that settled particles were recovered. The apparent size distributions of the 0.1 wt.% graphene concentration measured just after preparation and the 28th day are plotted in Figure 1.

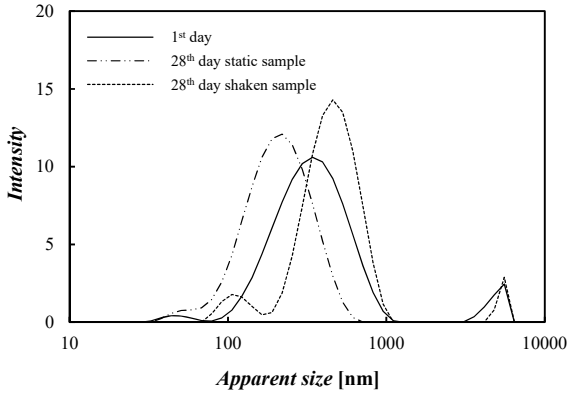

Figure 1 Apparent size distributions of the 0.1 wt.% GOnP/(EG+W) nanofluid.

As it can be observed, in the case of the static sample, the main peak slightly moves to left and the 4000-nm peak disappears while the 50-nm and 400-nm peaks move to the right for the shaken sample. This indicates a partial sedimentation ratio of the largest nanoparticles under static conditions.

Experimental methods

Thermal conductivities were determined by using a TPS 2500 S Hot Disk Thermal Analyzer® (Hot Disk AB, Sweden) together with a 7877 probe based on the Transient Plate Source (TPS) technique. The sensor was vertically immersed in the sample so that heat could freely diffuse in all directions. A delay of at least 15 min. was established between different measurements and both sample and probe were placed in a proper designed box and immersed in a thermostatic bath in order to ensure uniform initial temperature and remove thermal gradients. Analyses were performed by using low thermal powers, (40-55) mW, and short power input times, 4 s, with the object of minimizing possible convection effects. The thermal conductivity of water was also studied in the same temperature range and the results differ less than 1.5% from those of the NIST database [16]. These deviations are well within the uncertainties of the measurements. Additional information about the experimental device and measuring procedure can be found in Fedele et al. [23].

Rheological tests were performed by means of an AR-G2 magnetic bearing rheometer (TA Instruments, New Castle, USA) with a cone-plate geometry of 1° cone angle and 40 mm diameter. A Peltier plate and an upper heated plate (UHP) were utilized to regulate the sample temperature in the range from (293 to 343) K. Before experiments, the rheometer was carefully calibrated as further described by Bobbo et al. [24]. The geometry was imposed to a gap of 30 μm and an amount of 0.34 cm^3 was considered optimal for experiments. Flow curve analysis were carried out at constant temperature and shear rates ranging from (80 to 1200) s^{-1}. The dynamic viscosity of the water was also studied over the entire temperature range and the values exhibit an *AAD*s% less than 2% with those of the NIST database [16]. The estimated uncertainty of this device is less than 2% [24].

RESULTS AND DISCUSION

Thermal Conductivity

The influence of GnP concentration on the thermal conductivity was analyzed at temperatures ranging from (293 to 344) K with steps of 10 K. The temperature dependences of the different nanoparticle concentrations are depicted in Figure 2. Our thermal conductivities of base fluid were also compared with previous literature data. To our knowledge, only Melinder [11] reported values for the (EG+W) mixture at (10:90)% mass ratio. Additionally, Bohne et al. [25] and Sun et al. [26] studied different concentrations of this system and proposed correlations as functions of composition and temperature. The experimental results here presented exhibit *AAD*s% of 2.6, 4.0, and 1.9% with those reported or calculated by using those equations proposed by Melinder [11], Bohne et al. [25], and Sun et al. [26], respectively. Thermal conductivity rises with the addition of nanoplatelets reaching improvements of up to 5%. Enhancements are almost temperature-independent as previously reported in literature for graphene-nanofluids in EG [10] or EG+W [5] base fluids.

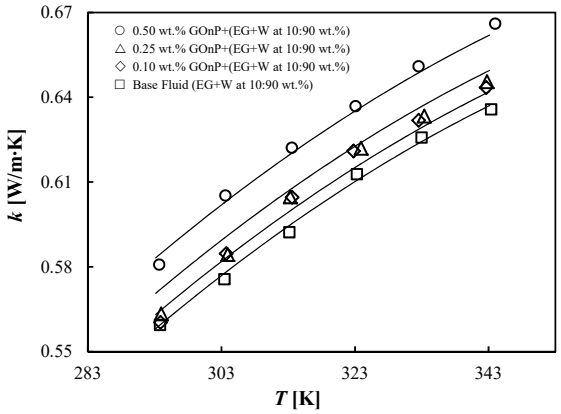

Figure 2 Temperature dependence of thermal conductivity, *k*, of GOnP/(EG+W) nanofluids. (—) Nan model [27], Eqs.(1-2).

Nan model [27] was used to describe the thermal conductivities of the studied nanofluid set. Nan et al. [27] generalized the Maxwell equation including the particle geometry effects and finite interfacial resistance through the following expression:

$$k_{nf} = k_{bf} \cdot \frac{3+\phi\cdot\left[2\cdot\beta_{11}\cdot(1-L_{11})+\beta_{33}\cdot(1-L_{33})\right]}{3-\phi\cdot\left(2\cdot\beta_{11}\cdot L_{11}+\cdot\beta_{33}\cdot L_{33}\right)} \quad (1)$$

where L_{ii} are the geometrical factors, which are L_{11}= 0 and L_{33}= 1 in the case of nanoplatelets [5, 19], ϕ is the nanoparticle volume fraction, and β_{ii} coefficients are defined as:

$$\beta_{ii} = \frac{k_{np}-k_{bf}}{k_{bf}+L_{ii}\cdot\left(k_{np}-k_{bf}\right)} \quad (2)$$

Our experimental results can be fitted with an *AAD*s%= 0.6% by using Eqs.(1-2) with a value of 17 W/m·K for the thermal conductivity of the nanomaterial, k_{np}.

Dynamic Viscosity

The rheological behavior of the base fluid and the three designed nanofluids was analyzed in the temperature range from (293.15 to 343.15) K. The comparison between the results obtained for the base fluid and previous literature data [11, 28-30] exhibit *AAD*s% from (1.5 to 3.6)%. Both base fluid and nanofluids are Newtonian over the studied concentration and shear rate range. This Newtonian behavior agrees with the results found by Kamatchi et al. [31] and Mehrali et al. [32] for graphene oxide-water nanofluids at shear rates higher than 80 s^{-1}. The temperature dependence of dynamic viscosity is plotted in Figure 3. As we can see, dynamic viscosity decreases considerably with temperature. The temperature behavior of this transport property can be described by utilizing the three-coefficient Vogel-Fulcher-Tamman (VFT) model:

$$\ln \eta(T) = \ln \eta_0 + \frac{D \cdot T_0}{T - T_0} \tag{3}$$

where η_0, D and T_0 are the adjustable coefficients. D and T_0 parameters are also known as the Angell Strength and Vogel temperature, respectively. As shown in Figure 3, this equation describes our experimental results with *AAD*s% lower than or equal to 1.6%. As expected, the addition of GOnPs raises the dynamic viscosity of nanofluids. This effect is more noticeable at high temperatures especially above 323.15 K, for which increases of up to 12.6% for the 0.5 wt.% GOnP mass concentration are reached.

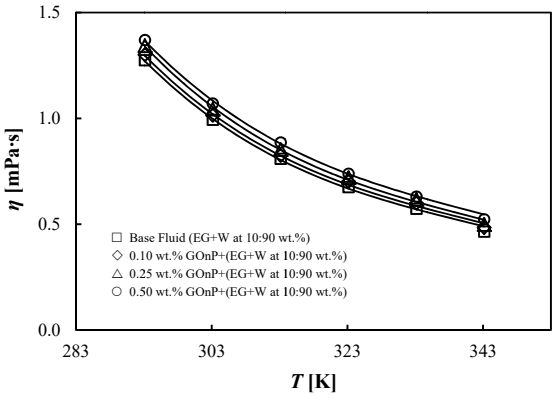

Figure 3 Temperature dependence of dynamic viscosity, η, of GOnP/(EG+W) nanofluids. (—) VFT model.

In the case of dispersions of non-interacting and stationary hard particles, relative viscosity can be described by means of the Einstein model [33]:

$$\frac{\eta_{nf}}{\eta_{bf}} = 1 + |\eta| \cdot \phi \tag{4}$$

where /η/ is known as intrinsic viscosity and quantifies the contribution of particle structure to the final viscosity of the suspension. /η/ depends on nanoparticle shape and takes a value of 2.5 for suspensions of mono-disperse and spherical particles and rises as shape differs from this spherical shape.
[34]. Maximum deviations less than 2.7% were found between experimental and correlated values by using Eq. (4) obtaining a value of 45 for /η/.

Nanofluid comparison based on thermophysical properties.

As indicated, different figures of merit can be utilized to assess the modification of heat transfer performance and pumping power of nanofluids regarding their base fluids.

Under laminar flow conditions, the replacement of the base fluid with a nanofluid would be beneficial in terms of energy when the increase in dynamic viscosity is less than four times the thermal conductivity enhancement [35]:

$$\frac{C_\eta}{C_k} = \frac{(\eta_{nf} - \eta_{bf})/\eta_{bf}}{(k_{nf} - k_{bf})/k_{bf}} \le 4 \tag{5}$$

Under turbulent flow conditions, the heat transfer performance can be assessed from the Mouromtseff number (*Mo*) [13] which is defined as:

$$Mo = \frac{\rho^{0.8} \cdot k^{0.67} \cdot c_p^{0.33}}{\eta^{0.47}}, \qquad \frac{Mo_{nf}}{Mo_{bf}} > 1 \tag{6}$$

A high *Mo* numbers indicates a good capability to transfer energy and so a high Mo_{nf}/Mo_{bf} ratio is desirable.

On the assumption that both base fluid and nanofluid have the same mass flow rates, the increase in pumping power in circular tubes with a boundary condition of uniform flux at the wall can be estimated by using the following expressions for laminar and turbulent flow conditions, respectively [36]:

$$\frac{\dot{W}_{nf}}{\dot{W}_{bf}} = \left(\frac{\eta_{nf}}{\eta_{bf}}\right) \cdot \left(\frac{\rho_{bf}}{\rho_{nf}}\right)^2 \tag{7}$$

$$\frac{\dot{W}_{nf}}{\dot{W}_{bf}} = \left(\frac{\eta_{nf}}{\eta_{bf}}\right)^{0.25} \cdot \left(\frac{\rho_{bf}}{\rho_{nf}}\right)^2 \tag{8}$$

Moderate $\dot{W}_{nf}/\dot{W}_{bf}$ ratios are preferred in order to avoid high increases in energy consumption because of fluid pumping.

In order to carry out these comparisons, the experimental dynamic viscosities and thermal conductivities here obtained were utilized, while density and specific heat capacity were calculated by using the following weighted average equations:

$$\rho_{nf} = \phi \cdot \rho_{np} + (1 - \phi) \cdot \rho_{bf} \tag{9}$$

$$c_{p,nf} = \varphi \cdot c_{p,np} + (1 - \varphi) \cdot c_{p,bf} \tag{10}$$

The values of density and heat capacity data were obtained from literature for nanoadditive [8] and base fluid [11]. The temperature dependences of these figures of merit (FOM) are plotted for the different studied nanofluids in Figure 4.

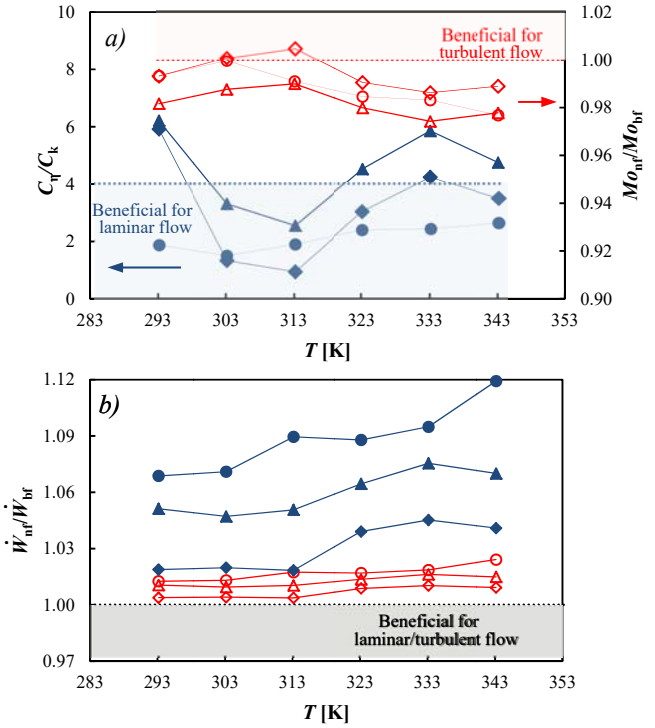

Figure 4 FOMs based on thermophysical properties for (◆,▲,◆) laminar and (◇,△,○) turbulent flow conditions. (◆,◇) 0.1, (▲,△) 0.25, and (●,○) 0.5 wt.% GOnP/(EG+W) nanofluids.

In the case of laminar flow conditions, only the highest studied concentration of nanoplatelets, 0.5 wtç%, would be advantageous in terms of thermal performance. However, for this same concentration under turbulent conditions the replacement would be beneficial only at temperatures of 303 and 313 K. On the other hand, the addition of GOnPs raises the pumping power up to 2.4% and 11.9% for turbulent and laminar flow conditions, respectively. As presented in Figure 4b, the increases in pumping power for both laminar and turbulent conditions are superior for the highest temperature since the increases in viscosity are also larger at those conditions.

CONCLUSIONS

New nanofluids were designed as dispersions of GOnPs in an (ethylene glycol + water) mixture and following a two-step process which was optimized by means of a stability analysis. Thermal conductivity and dynamic viscosity were experimentally obtained up to 0.5% nanoparticle mass concentrations. Despite the low concentrations utilized, thermal conductivity enhancements reach up to 5%. However, dynamic viscosity rises more strongly, especially at high temperatures, reaching a maximum increase of 12.6%. The temperature or nanoparticle behaviors of these two transport properties were also described by using Nan, Vogel-Fulcher-Tamman (VFT) or Einstein models with *AADs%* of 0.6%, 1.6%, and 1.3%, respectively. According to an analysis of different figures of merit based on the thermophysical properties of the nanofluids and base fluid, no significant increases in heat transfer performance would be expected under turbulent conditions for the studied nanoparticle range, while pumping power would rise up to 2.4% and 11.9% for turbulent and laminar flow conditions, respectively.

ACKNOWLEDGEMENTS:

This work was supported by the Ministerio de Economía y Competitividad (Spain) and the FEDER program through the ENE2014-55489-C2-2-R Project. Authors acknowledge the functionalized graphene nanoplatelets powder provided by Nanoinnova Technologies S.L. (www.nanoinnova.com). D.C. wants to thank the "Ministerio de Educación, Cultura y Deporte" (Spain) for a research stay grant under the FPU Program. Authors want to thank Antonella Barizza for her help in the measurements.

REFERENCES

[1] Mehrali, M.; Sadeghinezhad, E.; Rosen, M. A.; Akhiani, A. R.; Tahan Latibari, S.; Metselaar, H. S. C., Heat transfer and entropy generation for laminar forced convection flow of graphene nanoplatelets nanofluids in a horizontal tube, *International Communications in Heat and Mass Transfer*, Vol. 66, 2015, pp. 23-31.

[2] Park, E. J.; Park, S. D.; Bang, I. C.; Park, Y. B.; Park, H. W., Critical heat flux characteristics of nanofluids based on exfoliated graphite nanoplatelets (xGnPs), *Materials Letters*, Vol. 81, 2012, pp. 193-197.

[3] Lee, C.; Wei, X.; Kysar, J. W.; Hone, J., Measurement of the elastic properties and intrinsic strength of monolayer graphene, *Science*, Vol. 321, 2008, pp. 385-388.

[4] Balandin, A. A.; Ghosh, S.; Bao, W.; Calizo, I.; Teweldebrhan, D.; Miao, F.; Lau, C. N., Superior thermal conductivity of single-layer graphene, *Nano Letters*, Vol. 8, 2008, pp. 902-907.

[5] Kole, M.; Dey, T. K., Investigation of thermal conductivity, viscosity, and electrical conductivity of graphene based nanofluids, *Journal of Applied Physics*, Vol. 113, 2013, pp. 084307.

[6] Li, X.; Chen, Y.; Mo, S.; Jia, L.; Shao, X., Effect of surface modification on the stability and thermal conductivity of water-based SiO_2-coated graphene nanofluid, *Thermochimica Acta*, Vol. 595, 2014, pp. 6-10.

[7] Amiri, A.; Sadri, R.; Shanbedi, M.; Ahmadi, G.; Chew, B. T.; Kazi, S. N.; Dahari, M., Performance dependence of thermosyphon on the functionalization approaches: An experimental study on thermo-physical properties of graphene nanoplatelet-based water nanofluids, *Energy Conversion and Management*, Vol. 92, 2015, pp. 322-330.

[8] Pop, E.; Varshney, V.; Roy, A. K., Thermal properties of graphene: Fundamentals and applications, *MRS Bulletin*, Vol. 37, 2012, pp. 1273-1281.

[9] Teng, C. C.; Ma, C. C. M.; Lu, C. H.; Yang, S. Y.; Lee, S. H.; Hsiao, M. C.; Yen, M. Y.; Chiou, K. C.; Lee, T. M., Thermal conductivity and structure of non-covalent functionalized graphene/epoxy composites, *Carbon*, Vol. 49, 2011, pp. 5107-5116.

[10] Hadadian, M.; Goharshadi, E. K.; Youssefi, A., Electrical conductivity, thermal conductivity, and rheological properties of graphene oxide-based nanofluids, *Journal of Nanoparticle Research*, Vol. 16, 2014, pp. 2788.

[11] Melinder, A., Properties of secondary working fluids for indirect systems, *International Institute of Refrigeration (IIR)*, Paris, France, 2010

[12] Azmi, W. H.; Sharma, K. V.; Mamat, R.; Najafi, G.; Mohamad, M. S., The enhancement of effective thermal conductivity and

effective dynamic viscosity of nanofluids – A review, *Renewable and Sustainable Energy Reviews*, Vol. 53, 2016**,** pp. 1046-1058.
[13] Mouromtseff, I. E., Water and Forced-Air Cooling of Vacuum Tubes Nonelectronic Problems in Electronic Tubes, *Proceedings of the Institute of Electrical and Electronics Engineers (IEEE)*, New Yersey, USA, pp. 190–205.
[14] Cabaleiro, D.; Colla, L.; Agresti, F.; Lugo, L.; Fedele, L., Transport properties and heat transfer coefficients of ZnO/(ethylene glycol + water) nanofluids, *International Journal of Heat and Mass Transfer*, Vol. 89, 2015**,** pp. 433-443.
[15] Mehrali, M.; Sadeghinezhad, E.; Rosen, M. A.; Tahan Latibari, S.; Metselaar, H. S. C.; Kazi, S. N., Effect of specific surface area on convective heat transfer of graphene nanoplatelet aqueous nanofluids, *Experimental Thermal and Fluid Science*, Vol. 68, 2015**,** pp. 100-108.
[16] Lemmon, E. W.; Huber, M. L.; McLinden, M. O., NIST Standard Reference Database 23, in:, *Reference Fluid Thermodynamic and Transport Properties (REFPROP), National Institute of Standards and Technology*, Vol. 2010.
[17] Baby, T. T.; Ramaprabhu, S., Enhanced convective heat transfer using graphene dispersed nanofluids, *Nanoscale Research Letters*, Vol. 6, 2011**,** pp. 289.
[18] Jyothirmayee Aravind, S. S.; Ramaprabhu, S., Surfactant free graphene nanosheets based nanofluids by in-situ reduction of alkaline graphite oxide suspensions, *Journal of Applied Physics*, Vol. 110, 2011**,** pp. 124326.
[19] Yu, W.; Xie, H.; Wang, X., Significant thermal conductivity enhancement for nanofluids containing graphene nanosheets, *Physics Letters, Section A: General, Atomic and Solid State Physics*, Vol. 375, 2011**,** pp. 1323-1328.
[20] Amiri, A.; Sadri, R.; Shanbedi, M.; Ahmadi, G.; Kazi, S. N.; Chew, B. T.; Zubir, M. N. M., Synthesis of ethylene glycol-treated Graphene Nanoplatelets with one-pot, microwave-assisted functionalization for use as a high performance engine coolant, *Energy Conversion and Management*, Vol. 101, 2015**,** pp. 767-777.
[21] Ijam, A.; Saidur, R.; Ganesan, P.; Moradi Golsheikh, A., Stability, thermo-physical properties, and electrical conductivity of graphene oxide-deionized water/ethylene glycol based nanofluid, *International Journal of Heat and Mass Transfer*, Vol. 87, 2015**,** pp. 92-103.
[22] Fedele, L.; Colla, L.; Bobbo, S.; Barison, S.; Agresti, F., Experimental stability analysis of different water-based nanofluids, *Nanoscale Research Letters*, Vol. 6, 2011**,** pp. 300.
[23] Fedele, L.; Colla, L.; Bobbo, S., Viscosity and thermal conductivity measurements of water-based nanofluids containing titanium oxide nanoparticles, *International Journal of Refrigeration*, Vol. 35, 2012**,** pp. 1359-1366.
[24] Bobbo, S.; Fedele, L.; Benetti, A.; Colla, L.; Fabrizio, M.; Pagura, C.; Barison, S., Viscosity of water based SWCNH and TiO_2 nanofluids, *Experimental Thermal and Fluid Science*, Vol. 36, 2012**,** pp. 65-71.
[25] Bohne, D.; Fischer, S.; Obermeier, E., Thermal conductivity, density, viscosity, and Prandt-numbers of ethylene glycol-water mixtures, *Berichte der Bunsengesellschaft/Physical Chemistry Chemical Physics*, Vol. 88, 1984**,** pp. 739-742.
[26] Sun, T.; Teja, A. S., Density, viscosity, and thermal conductivity of aqueous ethylene, diethylene, and triethylene glycol mixtures between 290 K and 450 K, *Journal of Chemical and Engineering Data*, Vol. 48, 2003**,** pp. 198-202.
[27] Nan, C. W.; Birringer, R.; Clarke, D. R.; Gleiter, H., Effective thermal conductivity of particulate composites with interfacial thermal resistance, *Journal of Applied Physics*, Vol. 81, 1997**,** pp. 6692-6699.
[28] Tsierkezos, N. G.; Molinou, I. E., Thermodynamic properties of water + ethylene glycol at 283.15, 293.15, 303.15, and 313.15 K, *Journal of Chemical and Engineering Data*, Vol. 43, 1998**,** pp. 989-993.
[29] Yang, C.; Ma, P.; Jing, F.; Tang, D., Excess Molar Volumes, Viscosities, and Heat Capacities for the Mixtures of Ethylene Glycol + Water from 273.15 K to 353.15 K, *Journal of Chemical & Engineering Data*, Vol. 48, 2003**,** pp. 836-840.
[30] Iulian, O.; Ciocîrlan, O., Viscosity and density of systems with water, 1,4-dioxane and ethylene glycol between (293.15 and 313.15) K. I. binary systems, *Revue Roumaine de Chimie*, Vol. 55, 2010**,** pp. 45-53.
[31] Kamatchi, R.; Venkatachalapathy, S.; Abhinaya Srinivas, B., Synthesis, stability, transport properties, and surface wettability of reduced graphene oxide/water nanofluids, *International Journal of Thermal Sciences*, Vol. 97, 2015**,** pp. 17-25.
[32] Mehrali, M.; Sadeghinezhad, E.; Latibari, S.; Kazi, S.; Mehrali, M.; Zubir, M. N. B. M.; Metselaar, H. S., Investigation of thermal conductivity and rheological properties of nanofluids containing graphene nanoplatelets, *Nanoscale Research Letters*, Vol. 9, 2014**,** pp. 15.
[33] Einstein, A., A new determination of molecular dimensions, *Annals of Physics*, Vol. 19, 1906**,** pp. 289-306.
[34] Tesfai, W.; Singh, P.; Shatilla, Y.; Iqbal, M. Z.; Abdala, A. A., Rheology and microstructure of dilute graphene oxide suspension, *Journal of Nanoparticle Research*, Vol. 15, 2013**,** pp. 1989.
[35] Prasher, R.; Song, D.; Wang, J.; Phelan, P., Measurements of nanofluid viscosity and its implications for thermal applications, *Applied Physics Letters*, Vol. 89, 2006**,** pp. 133108.
[36] Mansour, R. B.; Galanis, N.; Nguyen, C. T., Effect of uncertainties in physical properties on forced convection heat transfer with nanofluids, *Applied Thermal Engineering*, Vol. 27, 2007**,** pp. 240-249.